Applied Microbiology and Biotechnology
https://doi.org/10.1007/s00253-019-09795-y

BIOTECHNOLOGICALLY RELEVANT ENZYMES AND PROTEINS

Exploring lectin-like activity of the S-layer protein of *Lactobacillus acidophilus* ATCC 4356

Joaquina Fina Martin[1,2] · Maria Mercedes Palomino[1,2] · Anabella M. Cutine[3] · Carlos P. Modenutti[1,2] · Dario A. Fernández Do Porto[1,2,4] · Mariana C. Allievi[1,2] · Sofia H. Zanini[1] · Karina V. Mariño[3] · Andrea A. Barquero[1,2] · Sandra M. Ruzal[1,2]

Received: 18 December 2018 / Revised: 22 March 2019 / Accepted: 23 March 2019

Abstract

The surface layer (S-layer) protein of *Lactobacillus acidophilus* is a crystalline array of self-assembling, proteinaceous subunits non-covalently bound to the outmost bacterial cell wall envelope and is involved in the adherence of bacteria to host cells. We have previously described that the S-layer protein of *L. acidophilus* possesses anti-viral and anti-bacterial properties. In this work, we extracted and purified S-layer proteins from *L. acidophilus* ATCC 4356 cells to study their interaction with cell wall components from prokaryotic (i.e., peptidoglycan and lipoteichoic acids) and eukaryotic origin (i.e., mucin and chitin), as well as with viruses, bacteria, yeast, and blood cells. Using chimeric S-layer fused to green fluorescent protein (GFP) from different parts of the protein, we analyzed their binding capacity. Our results show that the C-terminal part of the S-layer protein presents lectin-like activity, interacting with different glycoepitopes. We further demonstrate that lipoteichoic acid (LTA) serves as an anchor for the S-layer protein. Finally, a structure for the C-terminal part of S-layer and possible binding sites were predicted by a homology-based model.

Keywords S-layer · *Lactobacillus* · Lectin activity

Introduction

The surface layer protein (S-layer protein) of *Lactobacillus acidophilus* is a crystalline array of self-assembling, proteinaceous subunits, non-covalently bound to the outmost cell wall envelope. It plays a crucial role in biological functions by aiding adherence of the bacteria to host cells (Malamud et al. 2019). Notably, several but not all species of the genus *Lactobacillus* present S-layer proteins on their cell envelope (Allievi et al. 2019; Malamud et al. 2019). We have previously postulated that the S-layer protein of *L. acidophilus* acts as anti-viral and anti-bacterial candidate (Prado Acosta et al. 2008, 2016; Prado-Acosta et al. 2010; Martínez et al. 2012), as pre-treatment of the bacterial cells with purified S-layers not only reduced viability but also prevented infection of host cells (Martínez et al. 2012; Prado Acosta et al. 2016). Moreover, previous work has also shown that different S-layer proteins play a role both in the phenomena of exclusion of enteric pathogens (Hynönen et al. 2014; Meng et al. 2015; Zhu et al. 2016) and in the stimulation of the immune response via interactions with some intestinal epithelial cell components (Ashida et al. 2011; Carasi et al. 2014; Hymes and Klaenhammer 2016). Moreover, S-layer protein encoded by

J. Fina Martin and M. M. Palomino contributed equally to this work.

Electronic supplementary material The online version of this article (https://doi.org/10.1007/s00253-019-09795-y) contains supplementary material, which is available to authorized users.

✉ Sandra M. Ruzal
sandra@qb.fcen.uba.ar

[1] Facultad de Ciencias Exactas y Naturales, Departamento de Química Biológica, Universidad de Buenos Aires, Cdad. Universitaria, Pabellón II, 4 piso, Lab QB40, C1428EGA, CABA, Buenos Aires, Argentina

[2] Instituto de Química Biológica de la Facultad de Ciencias Exactas y Naturales (IQUIBICEN), CONICET-Universidad de Buenos Aires, Buenos Aires, Argentina

[3] Laboratorio de Glicómica Funcional y Molecular, Instituto de Biología y Medicina Experimental (IBYME), Consejo Nacional de Investigaciones Científicas y Técnicas (CONICET), C1428, Buenos Aires, Argentina

[4] Facultad de Ciencias Exactas y Naturales, Instituto de Cálculo, Universidad de Buenos Aires, Buenos Aires, Argentina

Published online: 03 May 2019

slpA gene (SlpA) of *L. acidophilus* NCFM was found to regulate dendritic and T cell functions by specific binding on their surface lectin receptor DC-SIGN (Konstantinov et al. 2008).

The S-layer protein contains a conserved N-terminal signal peptide of 25–30 amino acids (Palomino et al. 2016), indicative of its secretion via the general Sec-pathway. The primary sequence of the predominant S-layer, SlpA, of *L. acidophilus*, predicts a structural fold in two well-defined modules: the N-terminal part (amino acids 32 to 238) forms an external layer of protein monomers and interacts with the cell environment, while the C-terminal part (amino acids 239 to 444) is responsible for the cell wall anchorage (Smit et al. 2001; Smit and Pouwels 2002; Prado Acosta et al. 2008). Interestingly, the sequence of the N-terminal domain is variable, but the C-terminal domain is highly conserved in species of the *L. acidophilus* group, such as *Lactobacillus helveticus* and *Lactobacillus crispatus.* Based on electron microscopy, S-layer subunits exhibit lattices with oblique symmetry, permeable and with pores between the identical lattice units (Smit et al. 2001).

Similar to microbial adhesins, capable of recognizing oligosaccharides from glycoproteins either in the mucus layer or on the surface of epithelial cells in the gastrointestinal tract (van Tassell and Miller 2011), our in silico analysis revealed that the S-layer protein presents two carbohydrate recognition domains (CRD) probably responsible for glycoconjugate recognition in both prokaryotic and eukaryotic cells. (Martínez et al. 2012; Prado Acosta et al. 2016). Previous work (Johnson et al. 2013) has attributed adhesion capacity to the S-layer proteins, although this has not been thoroughly evaluated. In fact, it was shown that heterologous expression of a region of the S-layer from *L. brevis* conferred the ability to adhere to gut epithelial cells to a poorly adhesive lactic acid bacteria, i.e., *Lactococcus lactis* (Åvall-Jääskeläinen et al. 2003), highlighting a potential role of the S-layer protein in adhering to host cells.

Moreover, the C-terminal region of the *L. acidophilus* S-layer protein has been used to display heterologous proteins/epitopes (Smit and Pouwels 2002; Antikainen et al. 2002). However, there are still no details as to how the S-layer is anchored to the cell wall. In contrast to *Bacillus* and its relatives that contain S-layer homologous domains (SLH domains) involved in the anchoring of the S-layer to the cell wall components (Janesch et al. 2013; Sleytr et al. 2014; Allievi et al. 2014; Suhr et al. 2016; Blackler et al. 2018), such domains are not present in *Lactobacillus*. It has been described for the S-layer CbsA of *L. crispatus*, which shares 76% identity in primary sequence and in particular to the C-terminal region of the SlpA of *L. acidophilus*, that the protein binds to lipoteichoic acid (LTA) and functions to anchor the S-layer to the lactobacillar cell wall (Antikainen et al. 2002). Recent work in *Lactobacillus buchneri* shows that LTA mediates S-layer protein anchoring to the cell wall (Bönisch et al. 2018).

Considering that S-layer proteins contain two potential carbohydrate recognition domains (CRD) predicted in the C-terminal region of SlpA protein from in silico analysis (Smit et al. 2001; Martínez et al. 2012; Prado Acosta et al. 2016), we decided to study how the S-layer is anchored to the cell wall and how it exerts its anti-microbial effects, by analyzing the interaction with prokaryotic macromolecules such as peptidoglycan (PG) and lipoteichoic acids (LTA) and eukaryotic glycoconjugates, including glycoproteins, mucins, and polysaccharides such as chitin. To clarify the molecular mechanism by which the S-layer protein binds carbohydrates, we constructed chimerical GFP–S-layer fusion proteins with different parts of the *slpA* gene. A homology-based model to predict the structure of the C-terminal part is proposed and the most likely mechanism of interaction is discussed.

Materials and methods

Microorganism strains and growth conditions

L. acidophilus ATCC 4356, *L. helveticus* ATCC 12046, *Lactobacillus kefiri* JCM 5818, *Lactobacillus brevis* ATCC 14869, *Lactobacillus plantarum* ATCC 14917, and *Lactobacillus casei* BL23 were grown at 37 °C under static condition in de Man, Rogosa and Sharpe (MRS) medium. MRS medium (Biokar, Beauvais, France) pH = 6.5 contains 10 g/l tryptone, 4 g/l yeast extract, 8 g/l meat extract, 5 g/l Na acetate, 0.2 g/l $MgSO_4 \cdot 7H_2O$, 0.05 g/l $MnSO_4 \cdot 4H_2O$, 1 ml/l Tween 80, and 20 g/lglucose.

Escherichia coli Top10 (Thermo Fisher Scientific, Rockford IL, USA) was used for cloning, and *E. coli* HMS 174 (DE_3) (Novagen EMD Biosciences, Madison, WI, USA) was used for protein expression. *E. coli* strains were grown in LB (Luria Bertani) medium at 37 °C under aerated condition. When appropriate, antibiotics were added to the following concentrations: kanamycin, 30 μg/ml (Sigma, St Louis MO, USA) and ampicillin, 100 μg/ml (Sigma, St Louis MO, USA).

Bacillus cereus BGSC 6A1 (*Bacillus* Genetic Stock Center Columbus, OH, USA), *Pseudomonas aeruginosa* PAO 1, and *Salmonella enterica* serovar Newport ATCC 6962 (INEI-ANLIS Dr. Carlos G. Malbrán, Buenos Aires, Argentina) were grown in LB medium in aerated conditions at 37 °C for 16 h.

Saccharomyces cerevisiae NCYC 1115 was grown on rich medium containing 2% bactopeptone, 1% yeast extract, and 2% glucose (YPD) in aerated conditions at 30 °C for 16 h.

S-layer purification

Purified S-layer protein from *L. acidophilus* cultures grown in MRS medium at 37 °C was extracted by using a two-step LiCl extraction; first, with 1 M LiCl to release S-layer associated proteins (SLAP) (do Carmo et al. 2018), and then 5 M LiCl followed by extensive dialyzed against distilled water overnight at 4 °C and, after centrifugation (12,000*g*, 20 min),

resuspended in PBS (sterile phosphate-buffered saline) and stored at 4 °C (Palomino et al. 2016). Purity was checked by SDS-PAGE (Supplemental Fig. S1).

Hemagglutination and inhibition assays

Hemagglutination assays were adapted from (Sano and Ogawa 2014) and performed using 96-well microtiter plates with U-shape wells (Biofil, Guangzhou, China). Briefly, 50 μl of a twofold serial dilution of S-layer proteins (initial concentration: 1 mg/ml) in PBS was mixed with equal volume 4% (*v*/*v*) of sheep erythrocytes (Laboratorio Alfredo C. Gutiérrez Luján Buenos Aires Argentina http://www.alfredocgutierrez.com.ar/) and incubated for 1 h at room temperature. Formation of a reticulated suspension network indicates positive agglutinating activity, while a dot indicates negative agglutination.

For the hemagglutination inhibition assay, 1 mg/ml of S-layer protein was incubated with twofold serial dilution of carbohydrates, glycoproteins, or polysaccharides at room temperature for 1 h and then assayed for hemagglutination activity as described above.

To establish affinity of S-layer protein for carbohydrate structures, inhibition of hemagglutinating activity was tested using carbohydrate derivatives in solution (0.5 M in PBS).

Monosaccharides such as D-mannose, L-fucose, L-rhamnose, glucosamine, *N*-acetyl-D-glucosamine (NAG), D-glucose, D-galactose, disaccharide, D-lactose, all reagents were of analytical grade and purchased from Merck (Darmstadt, Germany) or Sigma-Aldrich (St Louis MO, USA). PBS and S-layer protein with no inhibitors were used as negative and positive controls respectively.

Bacterial agglutination

Exponential culture of *S. enterica* serovar Newport ATCC 6962, *P. aeruginosa* PAO 1, and *B. cereus* BGSC 6A1 were harvested and incubated at 37 °C for 1 h with S-layer or bovine serum albumin (BSA) as negative control. Cells were re-harvested and resuspended in milliQ water after incubation. LIVE/DEAD BacLight (Invitrogen, Eugene OR, USA) kit was used to visualize agglutination and cell death at the same time by fluorescence microscopy (Axiostar Plus; Carl Zeiss, Jena, Germany) with a × 100 objective with oil immersion. A suspension of only S-layer was visualized also as negative control.

Viral binding

We developed a strategy to assay viral binding, in analogy to pull-down procedures, taking advantage of the capacity of the S-layer suspension to aggregate and to precipitate when applying a low centrifugal force. Low centrifugal force does not precipitate virions due to their sedimentation coefficient that requires very high ultra-centrifugation forces (higher than 30,000×*g*) and time to form a pellet (Blanco Fernández et al. 2017). Human adenovirus type 5 (Adv-5 ATCC VR-1516), Herpes simplex type 1 (HSV-1 ATCC VR-1493), Vesicular Stomatitis Virus (VSV ATCC VR-1238), or phage J1 were incubated at 37 °C for 1 h with 400 μg/ml of S-layer suspension and centrifuged at 3800×*g* for 20 min. Aliquots of supernatant before and after centrifugation were serially diluted and titrated by plaque assay. A virus control was performed by incubating the virus suspension with PBS. With these data, the reduction factor (RF) was calculated as the logarithm of the ratio of viral titer before and after centrifugation in the virus control and treated with S-layer tubes. Inhibition of binding between S-layer and virus particles was assay by preincubation of the S-layer with 400 mM D-mannose. Virucidal activity of the S-layer was determined as described previously (Martínez et al. 2012) for all the viruses.

Dot-blot assay

Dot-blot assays were performed as previously described (Naughton et al. 2013) with some modifications. Macromolecules from different sources were immobilized onto a PVDF membrane (Thermo Scientific, Rockford IL, USA), including prokaryotic cell wall components and eukaryotic macromolecules: prokaryotic cell wall components: lipoteichoic acids (LTA), 20 mg/ml; peptidoglycan (PG), 20 mg/ml; cell wall polysaccharides (CWPS), 20 mg/ml; (prepared as described below); lipopolysaccharide (LPS), 6 mg/ml (Sigma, St Louis MO, USA); eukaryotic glycosylated proteins: stomach porcine mucin type III (PSM, 10 μg/ml) (Sigma, St Louis, USA), de-sialilated PSM (10 μg/ml); fibronectin (1 mg/ml) (Advanced Biomatrix, San Diego CA, USA), collagen (100 μg/ml) (Helena Laboratory Beaumont TX, USA); glucose oxidase (GOX, 2 μg/ml) (Sigma, St Louis MO, USA); fetuin (0.5 μg/ml) (Sigma, St Louis MO, USA); asialofetuin (0.5 μg/ml); RNAse B (5 μg/ml) (Sigma, St Louis MO, USA). Eukaryotic polysaccharides: chitin (30 mg/ml) (ICN Biomedicals Inc., Aurora OH, USA), chitosan (30 mg/ml) (Sigma, St Louis MO, USA), hyaluronic acid (HA, 2.5 mg/ml) (Sigma, St Louis MO, USA), and heparin (250 mg/ml) (Northia, Bs As, Argentina). Bovine serum albumin (BSA, 10 mg/ml) (Santa Cruz Biotechnology, Dallas TX, USA) was used as a negative control.

Desialylation of fetuin and PSM was done by incubating 2 h at 80 °C in acetic acid 2 N followed by neutralization with 5 M ammonium hydroxide. Finally, samples were dialyzed against water and concentrated.

After seeding, PVDF membranes were washed once and then blocked overnight at 4 °C in PBS containing 3% (*w*/*v*) BSA (Santa Cruz Biotechnology, Dallas TX, USA). Blocked membranes were washed and incubated at 37 °C for 1 h with an overlay with native S-layer-LiCl purified or fusion proteins

suspension (NT-GFP or GFP-CT) or GFP (50 μg/ml), the latter used as negative control. After incubating, membranes were washed three times with PBS Tween 20 0.05% *v*/*v* and positive dots were directly visualized by fluorescence in the case of GFP fusions, and then incubated with mouse polyclonal anti-S-layer antibodies (1:5000) (Prado Acosta et al. 2008). Binding was detected using HRP-conjugated anti-IgG mouse antibody (1:10000) and chemiluminescence using luminol substrate ECL (Amersham, GE Healthcare, Chicago, USA). Images were obtained with Amersham Imager 600 (GE Healthcare Bio-Sciences, Uppsala, Sweden). To determine concentrations of the blotted macromolecules, serial dilutions of known concentrations were spotted in PVDF and the spot with the minimum concentration assay was selected and shown in the figure.

Solid phase assay

Plate preparation for solid phase assay was performed as previously described (Carasi et al. 2014) with some modifications. In this assay, 96-well sterile polystyrene plates (Maxisorp Nunc, Roskilde, Denmark) were coated with mucin from porcine stomach type III (PSM, Sigma-Aldrich St Louis MO, USA) in PBS (50 μl, 10 mg/ml). Coating was achieved by incubation at 37 °C for 2 h, further overnight incubation at 4 °C, and a last incubation at 37 °C with increased volume (75 μl of 10 mg/ml PSM) to minimize empty binding sites. Finally, the plate was washed twice with PBS to eliminate excess of PSM. For the inhibition assay, S-layer (50 μg/ml) was pre-incubated at 37 °C for 2 h with inhibitors (D-galactose, D-glucose, D-mannose, and raffinose) and then incubated at 37 °C for 2 h in the PSM-coated plate. Each well was washed 3 times with PBS tween 0.05 % *v*/*v*, and then incubated with mouse polyclonal anti-S-layer antibody (1:5000) (Prado Acosta et al. 2008). Binding was detected using HRP-conjugated anti-IgG mouse antibody (1:10000) and 1-Step™ Turbo Tetramethylbenzidine (TMB)-ELISA substrate solution (Promega, Madison WI, USA). The reaction was stopped with sulfuric acid 1 M and absorbance was measured at 450 nm in a plate spectrophotometer. The IC_{50} values, concentration of sugar causing 50% inhibition of S-layer's binding to mucin, were calculated fitting log-transformed experimental data to a dose-response curve using GraphPad Prism® 5 for Windows software (Version 5.01, GraphPad Software, Inc., USA).

Cell wall (CW), peptidoglycan (PG), cell wall polysaccharides (CWPS), and lipoteichoic acids (LTA) extraction

Stationary phase cultures of *L. acidophilus* or *L. casei* were harvested by centrifugation and cells were washed with 50 mM Tris/HCl pH 7.5.

LTA was purified from *L. acidophilus* by extraction with 1-butanol (Palomino et al. 2013). S-layer protein was purified as described above (Palomino et al. 2016). To purify CW and PG, bacterial cells were treated as previously described (Piuri et al. 2005; Palomino et al. 2013).

CWPS from *L. casei* where obtained with trichloroacetic acid (TCA) treatment. TCA-extracted walls were prepared with CW by treatment with 10% (*w*/*v*) TCA for 48 h at 48 °C followed by extensive washing with cold deionized water (de Ambrosini et al. 1996). CWPS were collected in the insoluble fraction.

Molecular cloning and plasmid construction

A C-terminal green fluorescent protein (GPF) fusion expression vector was constructed, amplifying *gfp* from pM14 (Piuri et al. 2009) with the following primers:

GFP1-5′TGCGTCGACATGGTGAGCAAGG-3′

GFP2-5′TGGCTCGAGCTTGTACAGCTCGTCC-3′

(the underlined letters correspond to restriction sites).

The PCR product was digested with *Sal*I and *Xho*I and cloned into pET21b (Novagen, EMD Biosciences, Madison, WI, USA) to generate pET21-GFP vector. The pET28-GFP was used as N-terminal GFP fusion expression vector (Dieterle et al. 2014).

All DNA sequences were amplified by PCR using Go Taq DNA polymerase (Promega, Madison, WI, USA) by following the manufacturer's instructions.

Different *slpA* regions were amplified using chromosomal DNA of *L. acidophilus* as template, amplified using the primers described in the Table 1, and cloned into pET21-GFP. Figure 4 a shows different SlpA regions analyzed.

Protein purification

Plasmids described above were transformed into *E. coli* HMS 174(DE3) cells (Novagen, EMD Biosciences, Madison, WI, USA) by electroporation for protein expression and further purification. Transformed cells were grown with aeration at 37 °C to an OD600 of 0.5 in LB medium. Protein expression was induced by adding 0.1 mM isopropyl-β-D-thiogalactopyranoside (IPTG) and the cultures were further incubated overnight at 19 °C before being harvested. Cell pellets were resuspended in binding buffer (50 mM Tris-HCl [pH 8], 300 mM NaCl, and 1 mM phenylmethylsulfonyl fluoride [PMSF]) and disrupted by sonication (6 cycles of 15 s). The clear lysates were centrifuged at 12,000×*g* for 20 min, and the supernatants were filtered (0.22 μm Millipore Burlington, MA, USA) to remove the cell debris.

Subsequently, the clear lysates were applied to HisTrap™ HP columns (GE Healthcare, Uppsala, Sweden) equilibrated with the binding buffer (20 mM sodium phosphate, 500 mM NaCl, 25 mM imidazole, pH 7.4), then the columns were

Table 1 Primers used for GFP chimeric constructions

Chimeric constructions	Forward primer[1]	Reverse primer[1]
NT-GFP cloned into pET21-GFP	TGGCATATGGCTACTACTATTAA CGCA (*Nde*I restriction site)	CGTGTCGACAGTGAAAGTATGAGG (*Sal*I restriction site)
GFP-CT1 cloned into pET28-GFP	AGTGGATCCAACGTTAAAGCAAC (*Bam*HI restriction site)	TAGGAGCTCTAATCTAAAGTTTGC (*Sac*I restriction site)
GFP-CT2 cloned into pET28-GFP	AGTGGATCCATGCACAACGCATAC (*Bam*HI restriction site)	TAGGAGCTCTAATCTAAAGTTTGC (*Sac*I restriction site)
GFP-CT3 cloned into pET28-GFP	AGTGGATCCATGCACAACGCATAC (*Bam*HI restriction site),	TAGGAGCTCTTAGTTTGCAG CGTTGATG (*Sac*I restriction site)
GFP-CT4 cloned into pET28-GFP	AGTGAATTCTTTGCAGCACAATA CGC (*Eco*RI restriction site)	TAGGAGCTCTTATCTAAAGTTTGC (*Sac*I restriction site)
GFP-CT5 cloned into pET28-GFP	AGTGAATTCTTTGCAGCACAATA CGC (*Eco*RI restriction site)	TAGGAGCTCTTAGTTTGCAGCGT TGATG (*Sac*I restriction site)

[1] Restriction sites in primers are underlined

washed with washing buffer (20 mM sodium phosphate, 500 mM NaCl, 50 mM imidazole, pH 7.4) and the His-tagged protein was eluted in elution buffer (20 mM sodium phosphate, 500 mM NaCl, 200 mM imidazole, pH 7.4). Eluted samples were dialyzed twice against protein buffer (50 mM Tris-HCl [pH 8], 150 mM NaCl, 1 mM dithiothreitol [DTT]) and once again in the same buffer with 30% glycerol and then stored at − 20 °C.

Protein concentration was determined at 280 nm in a Nanodrop 2000 Spectrophotometer (Thermo Scientific, Madison, WI, USA) or Metrolab 1700 UV/Vis Spectrophotometer (Metrolab, Buenos Aires, Argentina) and the molar extinction coefficients were calculated using Expasy's ProtParam tool (https://web.expasy.org/protparam/). SDS-PAGE was used to analyze protein expression.

The binding of SlpA fusion proteins to *L. acidophilus*

L. acidophilus cultures were grown as mentioned above; cells were harvested in the stationary phase. After treating with 5 M LiCl to remove S-layer protein, cells were washed twice and resuspended in phosphate-buffered saline (PBS) adjusting to an OD600 of 1.0.

In a typical binding experiment, aliquots of 300 μl of culture were incubated for 60 min at 37 °C with 10 μg of SlpA NT-GFP, GFP-CT1 chimerical fusion proteins. GFP purified protein and PBS were used as negative and autofluorescence controls respectively. After binding, cells were collected by centrifugation at 10,000×*g* for 5 min and washed twice. Cells were resuspended in 100 μl of PBS and whole cells bound with SlpA fusion proteins were analyzed by fluorescence microscopy (Axiostar Plus; Carl Zeiss, Jena, Germany) with a × 100 objective with oil immersion, and phase contrast and flow cytometry techniques. For the latter method, after the binding assay, the mixture was washed twice with PBS and resuspended in 300 μl of PBS with approximately 1×10^6 cells. Fluorescent and non-fluorescent cells within the gated population were distinguished based on fluorescent intensity (GFP-H). BD FACSAria software (BD FACSDiva, firmware version 6.1.3; BD Bioscience, San Jose, CA) was used for data acquisition, and FlowJo 10.0.7 software (https://www.flowjo.com/) was used for subsequent analysis. Assays were carried out on triplicate and data were normalized to the means for three replicates.

Competitive inhibitors of SlpA binding to *L. acidophilus* were tested with increasing concentrations of monosaccharides such as D-mannose, D-fructose, glucosamine, *N*-acetyl-D-glucosamine (NAG), *N*-acetylneuraminic acid, D-glucose, D-galactose, L-fucose, and L-rhamnose; the disaccharide D-lactose and trisaccharide raffinose (*O*-α-D-galactopyranosyl-(1 → 6)-α-D-glucopyranosyl β-D-fructofuranoside) or *N*-acetylneuraminyllactose (sialyllactose) (Elicityl, Crolles, France) (concentration range micromolar to millimolar) and polymers, chitin, or LTA; all reagents were of analytical grade and purchased from Merck (Darmstadt, Germany) or Sigma-Aldrich (St Louis MO, USA) unless stated otherwise. For polymers, concentrations in nanomoles was calculated based on their monomer content in an average chain length as reported in previous literature; for chitin, chain length was estimated in 900 monomers (203 g/mol monomer NAG) (Howling et al. 2001), and for LTA, an average chain length of 27.5 (172 g/mol monomer glycerol phosphate) was estimated (Cleveland et al. 1975), considering data from *L. helveticus* DSM 20075T and *L. buchneri* CD034, both strains harboring S-layer proteins (Shiraishi et al. 2016; Bönisch et al. 2018).

Purified LTA were pre-incubated with anti-LTA antibody before the inhibition assay.

Cells were subjected to different treatments to identify the cell wall components responsible for S-layer interaction. Treatment included chelating agents 10 mM (EDTA, Sigma, St Louis MO, USA) trichloroacetic acid 10% (TCA),

mutanolysin 100 U/ml (Sigma, St Louis MO, USA), and sodium dodecyl sulfate 10% (SDS, Sigma, St Louis MO, USA)

Lectin blot

Preparations of S-layer protein (30 μg) and RNase B (4 μg), were heated at 90 °C for 5 min in loading buffer (10% glycerol, 4% sodium dodecyl sulfate (SDS), 4 M urea, 2% β-mercaptoethanol, and 0.05% bromophenol blue) and subjected to electrophoresis in 12.5% SDS-PAGE. For lectin blot analysis, proteins were electrotransferred with a semi-dryblotter (Amersham Biosciences, Chicago, USA) to PVDF membranes (Macherey-Nagel, Düren, Germany). Then, the membrane was stained with Ponceau S stain to corroborate that the transfer was efficient or blocked 1 h RT with TBS-Tween 20 0.1% *v*/*v*-BSA 3% *w*/*v* to continue with the lectin blot. Later, membranes were washed three times with TBS-Tween 20 0,1% *v*/*v* and incubated 30 min RT with biotin-conjugated concanavalin A (ConA) (1 μg/ml, Vector Labs, Burlingame, USA) with or without 200 mM methyl α-D-mannoside and methyl α-D-glucoside inhibitors. After washing three times, membranes were incubated 1 h at room temperature with HRP-conjugated streptavidin (0.5 μg/ml Sigma, St Louis MO, USA). Lastly, chemiluminescence was detected with luminol substrate ECL (Amersham, GE Healthcare, Chicago, USA). Images were obtained with an Amersham Imager 600 (GE Healthcare Bio-Sciences AB, Uppsala, Sweden).

The glycosylation of the protein was also evaluated using Thermo Scientific Pierce (Rockford IL, USA) Glycoprotein Staining Kit following the manufacturer's instructions.

Computational methods: comparative modeling

Template search was done using the HHpred tool of the Max Planck Institute Bioinformatics Toolkit (Alva et al. 2016). We employed two different templates to build the S-layer model, one coming from a *Staphylococcus epidermidis* structure (PDB id: 4EPC, identity: 27%) and other coming from a *S. cerevisiae* structure (PDB 3 U28, identity: 31%)

More than one thousand models were generated using the Modeller v.9.19 software (Eswar et al. 2008). All models were manually inspected to select those that conserved typical native contacts in similar protein folding.

Molecular dynamics simulations

As the modeled protein has a low identity against the chosen template, we refined the structure using molecular dynamics simulations as described previously by Blanco Capurro et al. (2019).

Pocket analysis

Structural druggability of each potential pocket was assessed by determining (and characterizing) the ability to bind a drug-like molecule by using the fpocket program (Le Guilloux et al. 2009). Briefly, the method is based on Voronoi tessellation algorithm to identify pockets and computes suitable for physicochemical descriptors (polar and apolar surface area, hydrophobic density, hydrophobic, and polarity score) that are combined to yield the Druggability Score, which ranges from 0 (non-druggable) to 1 (highly druggable) (Sosa et al. 2018).

Fluorescence spectroscopy

The interaction of S-layer with carbohydrates was monitored by changes in fluorescence intensity and λmax of the protein resulting from binding of carbohydrates. The fluorescence emission spectra are recorded at room temperature, from 290 to 380 nm, with an excitation wavelength of 275 nm and emission at 305 nm in quartz cuvettes of 10 mm optical path. A Cary eclipse fluorescence spectrometer (AMINCO-Bowman, series 2, Thermo Scientific, Madison, WI, USA) with 8-nm bandpass filter was used. Titrations were carried out by adding 1-μl aliquots of carbohydrates stock (0.5 M) or chitin hydrolysate (Vector Labs, Burlingame, USA) in PBS to 0.2 ml of purified S-layer protein 0.5 mg/ml in PBS. The fluorescence of each sample was measured, the sugar concentration varying from 0 to 20 mM. Each spectrum was an average of three successive scans, and no correction for dilution effect due to the addition of carbohydrate solutions was needed, since added volume did not exceed 10% of the total volume. Fluorescence spectroscopy allows quenching to be described by means of the Stern-Volmer equation. $F_0/F = 1 + K_a[AF]$, where F_0 and F are the fluorescence emission intensities in the absence and presence of sugar respectively, [AF] is the sugar concentration, and K_a is a constant equal to the reciprocal of the sugar concentration when the fluorescence intensity decreases by half. The final value of K_d was calculated from three independent readings and represented as an average of final K_d values along with the standard error mean, calculated from standard deviation (Bose et al. 2016; Patel et al. 2016).

Statistical analysis

Assays were carried out on triplicate and data were normalized to the means for three replicates. Results are presented as means ± standard deviations (indicated by error bars) for replicate experiments. The one-way analysis of variance (ANOVA) followed by Bonferroni post hoc test was used to estimate statistical significance; a P value of < 0.05 was considered significant.

Results

L. acidophilus S-layer protein has the capacity to agglutinate blood cells and bacteria

We tested hemagglutination, a simple and easy method to obtain semi-quantitative data on the binding to carbohydrates and a first insight on the lectin specificity, as an initial step to characterize the lectin-like activity of the S-layer protein (Sano and Ogawa 2014). We optimized the protocol and established an S-layer protein minimum concentration of 250 μg/ml for the agglutination of sheep red blood cells. To further characterize the glycoepitopes mediating hemagglutination, we tested different carbohydrate derivatives as potential inhibitors, including several disaccharides and monosaccharides (D-lactose, D-maltose, D-glucose, D-mannose, D-galactose, L-rhamnose, L-fucose, glucosamine, and *N*-acetyl-D-glucosamine), although a poor inhibitor, D-mannose, was the best monosaccharide tested with a minimal inhibitory concentration (MIC) of 15 mM, as other monosaccharides required from a fivefold to a tenfold increase in concentration (D-glucose MIC = 1 M, L-fucose MIC = 0.5 M, D-galactose MIC = 0.25 M L-rhamnose MIC = 0.125 M). Competitive inhibition was also evident with disaccharide D-lactose (MIC = 15 mM) and PSM (MIC = 0.15 mg/ml), but when testing polymers, chitin and chitosan, they showed an intrinsic hemagglutinating capacity, so they could not be evaluated.

Bacterial clumping (agglutination) makes it possible to recognize interactions that occur when a protein with lectin activity is added to a bacterial suspension. Specific interactions of the S-layer protein with Gram-positive/Gram-negative bacteria and yeast cells were evaluated by agglutinating activity (Fig. 1). LiCl purified S-layer protein was able to agglutinate yeast cells, probably based on the presence of mannose-containing polysaccharides in the cell wall of *S. cerevisiae* and with Gram-negative *S. enterica* and *P. aeruginosa* due to interactions with LPS in the outer membrane. Agglutination was also evident with Gram-positive *B. cereus* probably based on the interaction with cell wall polymers. Notably, bacterial agglutination increased the number of dead cells (showed by red fluorescence using Live-Dead fluorophore), which correlates with the anti-microbial activity reported for the S-layer protein (Fig. 1) (Prado Acosta et al. 2008; Martínez et al. 2012; Hynönen et al. 2014; Meng et al. 2015; Prado Acosta et al. 2016; Zhu et al. 2016).

S-layer interacts with eukaryotic and prokaryotic macromolecules and viruses

Dot-blot assays were used to determine which components are involved in the interaction with LiCl purified S-layer protein. In accordance with the results previously described for other S-layers (Panwar et al. 2017; Antikainen et al. 2002; Åvall-Jääskeläinen et al. 2008; Zhu et al. 2016), both chitin and chitosan are ligands for S-layer protein SlpA. Moreover, different fractions of the Gram-positive envelope (PG and LTA from *L. acidophilus*) showed binding although with less affinity to CWPS from *L. casei* (Fig. 2).

Eukaryotic glycoproteins (PSM, fibronectin, collagen, glucose oxidase, fetuin, RNAse B) and polysaccharides (hyaluronic acid) were also assayed. BSA was used as a negative control since it is not glycosylated (Fig. 2). From all glycoproteins evaluated, PSM and fetuin, both having a variable degree of sialylation (Windwarder and Altmann 2014; Nishiyama et al. 2016), were ligands for S-layer protein, but, notably, RNAse B and glucose oxidase, both containing high mannose glycans (Domurado et al. 1995), were not recognized by the S-layer protein. Given these results, we tested desialylated PSM and fetuin binding that decreased considerably. Binding to PSM and fetuin and decrease upon desialylation indicates sialic acid recognition, but it seems it is not the only one: a wide range of binding affinity to various polymers was observed also including chitin and chitosan, and hyaluronic acid, Gram-positive PG and LTA.

We optimized a solid phase assay based on the affinity of SlpA for PSM and examined different glycostructures as inhibitors of this binding in a competitive manner. D-mannose inhibited the interaction of SlpA with PSM with low affinity (D-mannose IC_{50} =59 mM, Supplemental Fig. S2), while D-glucose, D-galactose, and D-lactose showed very poor interactions and higher IC_{50} values, ranging from 150 to 200 mM. The trisaccharide carbohydrate (raffinose) was used as a control with no inhibitory effect.

Additionally, binding to viral particles was evaluated by pull-down assays. S-layer proteins extracted with 5 M LiCl from intact cells interacted with each other to produce a paracrystalline array suspension upon removal of lithium salts by dialysis, forming a white precipitate that could be recovered by centrifugation. After centrifugation, intact purified S-layer (400 μg/ml) showed the decrease in viral titer in pull-down assay: a two-log decrease in viral title was obtained for Adv-5, HSV-1, and VSV viruses, while no interaction was observed with bacteriophage J1 particles (Fig. 3a). No virucidal activity was observed for the S-layer that could justify that decrease (Fig. 3b). These results suggested that S-layer protein could have a direct interaction with animal viruses probably through carbohydrate patterns. To test carbohydrate's involvement in that interaction, we assayed the inhibition effect of D-mannose on the pull-down titer reduction with the complex virus particle HSV-1 that possesses an envelope with different glycoproteins. The S-layer dependent decrease in viral titer described in Fig. 3a was significantly inhibited (67%) by preincubation of the S-layer with 400 mM D-mannose before allowing the interaction with HSV-1. D-mannose did not have any effect on the replication of HSV-1. The inhibition of pull-down of virus particles by addition of D-mannose together with the absence of a pull-down effect on bacteriophage particles, known to lack glycoproteins

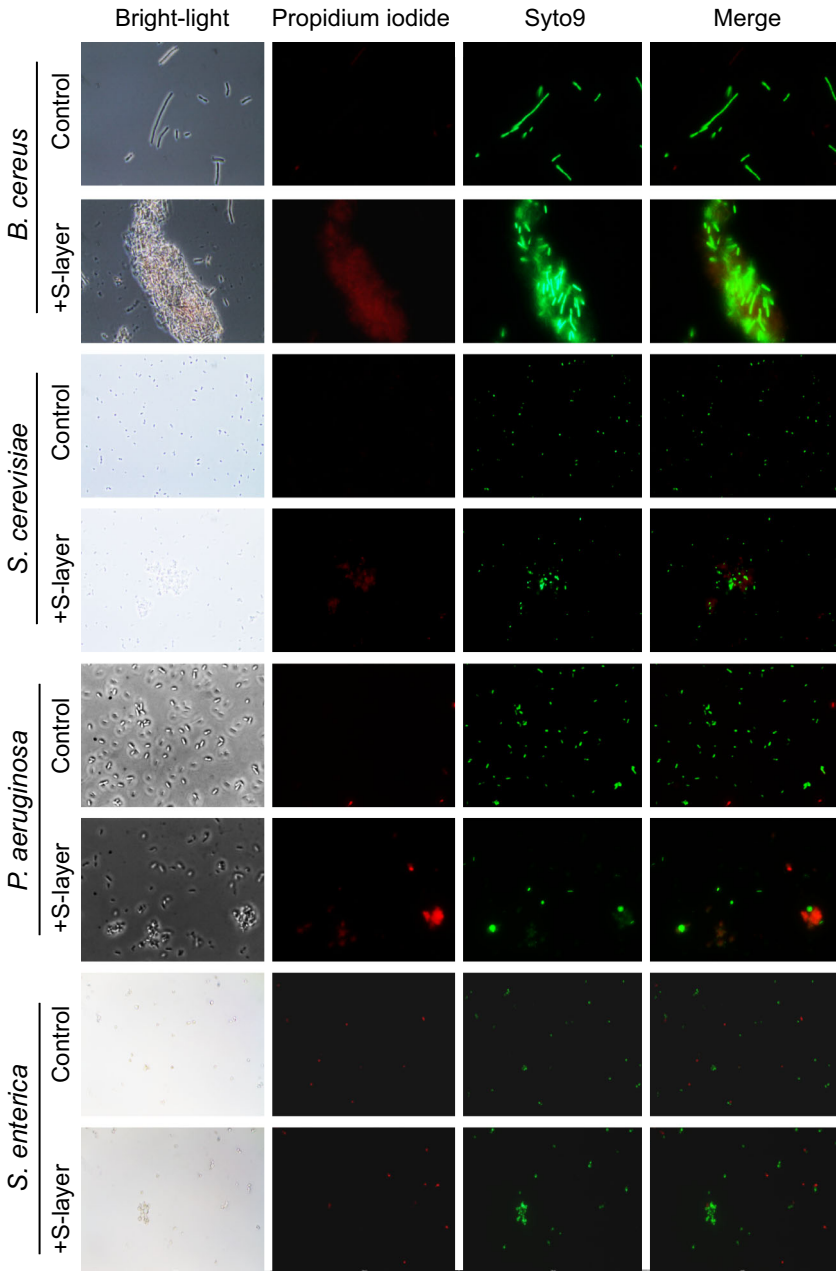

Fig. 1 Agglutination of *Bacillus cereus* (magnification, × 1000), *Salmonella enterica* (magnification, × 1000), *Pseudomonas aeruginosa* (magnification, × 1000), and *Saccharomyces cerevisiae* (magnification, × 400). Cells without added S-layer did not agglutinate (control). Agglutination in the presence of S-layer (+S-layer) was visualized by bright-light microscopy and Live-Dead fluorescence (propidium iodide and Syto 9)

in their capsids, suggested an involvement of carbohydrate recognition domains of the S-layer in the interaction with viral glycosylated components.

Functional analysis of the N- and C-terminal parts of the S-layer in carbohydrate binding

As we described above, carbohydrate recognition domains (CRD) are predicted in the C-terminal region of the SlpA protein (Smit et al. 2001; Martínez et al. 2012; Prado Acosta et al. 2016). Two internal repeats are found in the C-terminal part of the S-layer protein, 57 and 58 amino acids long, with 60% similarity and 26% identity, most of which are basic and aromatic amino acids (Fig. 4b). A consensus sequence described by von Eichel-Streiber for *Clostridium difficile* toxins (ToxA) (Ho et al. 2005) and *Streptococcus mutans* glucosyltransferases (GBP) (von Eichel-Streiber et al. 1992) is found within the repeats. At the beginning of each internal repeat, a five amino acid sequence similar to those found in mannose-binding lectins (MBL) was detected (An et al. 2006) (Fig. 4b).

To characterize the minimum amino acid sequence of SlpA required for binding, we constructed chimerical fusions to the green fluorescent protein (GFP) containing different peptides of the S-layer protein SlpA (Fig. 4a) and assessed them for GFP-tagged binding. GFP tagging was located upstream of

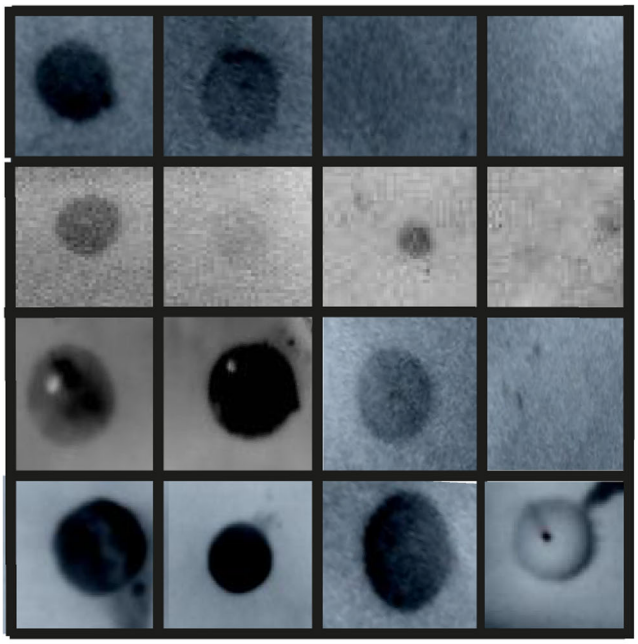

Collagen 3 μg	Fibronectin 20 μg	RNase B 20 μg	GOX 6 μg
PSM 10 μg	PSM not sialylated 10 μg	Fetuin 0.5 μg	Fetuin non *N*-gly 0.5 μg
Chitin 30 μg	Chitosan 30 μg	HA 25 μg	BSA 10 μg
PG L ac 50 μg	PG BL23 50 μg	LTA 50 μg	CWPS 50 μg

Fig. 2 The binding capacity of the S-layer protein to prokaryotic cell wall components and eukaryotic macromolecules was verified by dot-blot assay (upper) and representative diagram of the immobilized components in the PDVF membrane is shown (lower)

the C-terminal part of SlpA or downstream of the N-terminal to maintain the native configuration in the S-layer protein. Binding capacity was verified by dot-blot analysis and visualized by fluorescence binding assays. We found that the C-terminal part of the SlpA protein (GFP-CT1, 2 and 4) interacts with polymers including Gram-negative LPS and Gram-positive cell wall components (PG, LTA, and CWPS) and eukaryotic macromolecules (mucin, hyaluronic acid) and polymeric carbohydrates (chitin and chitosan), but no interaction was observed when one internal repeat was absent (GFP-CT3 and 5). Therefore, both internal repeats are necessary for the interaction with the cell wall (Fig. 4a). This is in accordance with the need of multiple binding sites like those found on ToxA or GBP protein along the length of their carboxy termini that may strengthen binding to carbohydrates (Greco et al. 2006). The only interaction observed for the N-terminal part was with fibronectin and collagen as well as with the S-layer itself (Fig. 4a)

GFP-CT fluorescence binding assays

In order to study the interaction of S-layer proteins and to quantify and compare the binding strength with whole lactobacillar cells, they were analyzed by fluorescence microscopy and flow cytometry (Fig. 5a-c) using the chimeric protein GFP-CT1 described in Fig. 4a. Binding of GFP-CT1 was inhibited by the addition of lipoteichoic acid (LTA), and monosaccharides. As shown in Fig. 5, the binding of carboxy termini to whole cells was also inhibited by the presence of different glycostructures. Absence of binding to whole cells was obtained for NT-GFP.

Relative fluorescence in the presence of increasing concentration was plotted (Fig. 5d), and an IC_{50} (concentration causing 50% inhibition of binding) was calculated from the plots being micromolar for polymeric compounds (0.09 μM for LTA and 0.15 μM for chitin) and millimolar for other monomeric or dimeric carbohydrates (0.3 mM *N*-acetylneuraminic acid, 0.5 mM α-2,3-sialyllactose, 2.5 mM for D-mannose, D-lactose 5.5 mM, D-fructose 129 mM, 134 mM for D-glucose, and 237 mM for D-galactose). Considering the higher affinity for negatively charged polymers such as LTA, we also evaluated if phosphorylated monosaccharides showed an increased affinity. However, no difference was observed (data not shown) suggesting that increasing negative charges in the carbohydrate molecules do not increase binding.

Interestingly, GFP-CT1 showed low binding to other *Lactobacillus* cells including *L. casei* and *L. plantarum*, which do not possess S-layer (Fig. 6a). Moreover, pre-growth in high salt medium decreased binding of the GFP-CT1 fusion protein, indicating that, in a similar manner to what was observed for *L. casei* BL23, cell wall modifications arise in high-salt conditions (Piuri et al. 2005; Palomino et al. 2013).

To identify the cell wall components responsible for S-layer attachment, cells were differentially treated in order to verify which component was involved in the interaction. Treatment included trichloroacetic acid (TCA) to remove cell wall linked teichoic acids (WTA), while mutanolysin treatment was intended to remove PG and WTA, leaving detergent (SDS) treatment to remove LTA. As shown in Fig. 6b, no difference was observed for EDTA, TCA, or mutanolysin treatments, while SDS dramatically decreased the GFP-CT1 interaction and served to differentiate interaction between WTA from membrane anchored LTA. Furthermore, when purified LTA was pre-incubated with anti-LTA antibody before the inhibition assay, it increased binding, indicating a specific interaction between LTA polymer and GFP-CT1 protein in the cell surface (Fig. 6b).

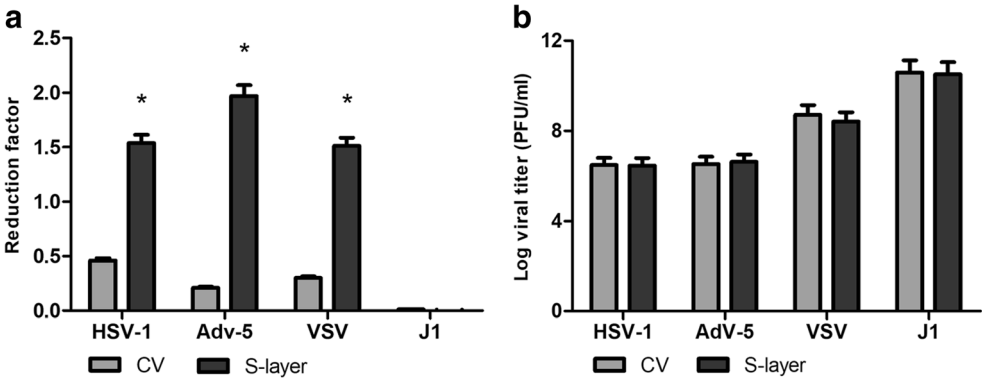

Fig. 3 **a** Viral binding assay: the interaction between viruses HSV-1, Adv-5, VSV, or phage J1 with the purified S-layer suspension (400 μg/ml) was evaluated. Results of virus titration in plaque assay are given with (S-layer) and without S-layer (Control virus: CV). The asterisk (*) denotes significant difference with respect to the control using the ANOVA method, Bonferroni test ($p < 0.05$). **b** Evaluation of virucidal activity. Control virus (CV) and S-layer. There was no significant difference with respect to the control using the ANOVA method, Bonferroni test ($p < 0.05$)

Glycosylation of S-layer protein

Lactobacillus S-layer proteins were generally considered to be non-glycosylated. However, studies of the S-layer from *L. kefiri* (Cavallero et al. 2017) and *L. buchneri* (Anzengruber et al. 2014) have shown them to be glycosylated. Controversy arises for *L. acidophilus* strains since SlpA in *L. acidophilus* NCFM was suggested to be glycosylated, through experiments with specific lectins assayed by ELISA (Konstantinov et al. 2008), although staining of SlpA protein of *L. acidophilus* ATCC 4356 was not completely conclusive (Martínez et al. 2012; Prado Acosta et al. 2016). To solve this difference, a lectin blot with ConA, a lectin that recognizes high mannose residues, was performed. ConA was able to specifically recognize native S-layer protein indicating that it is glycosylated (Supplemental Fig. S3A). Nine characteristic sequons (Asn-X-Ser/Thr) for *N*-linked oligosaccharides are present in the S-layer amino acid sequence, 8 in the N-terminal and one in the C-terminal part of mature SlpA (Supplemental Fig. S3B).

C-terminal structure model

Although definite 3D structure of a lactobacilli S-layer protein has not yet been solved, bioinformatic modeling is an alternative method to predict the structure of the C-terminal part and try to identify possible binding sites. A homology-based model was built using as a template the *N*-acetylmuramoyl-L-alanine amidase, Atl (PDB id 4EPC), the major murein hydrolase involved in cell separation, which repeats are able to bind to LTA as an anchor for the Atl (Zoll et al. 2012). The structure model is presented in Fig. 7a including the residues that are components of the most probable binding site (FPocket Druggability Score of 0.768) (Sosa et al. 2018). The volume of the pocket is approximately 564 Å, enough to harbor two hexoses with individual volumes of 216 Å.

Fluorescence quenching of tyrosines

The fluorescence emission spectra of S-layer protein showed a λmax of 304 nm when excited at 275 nm due to the predominant presence of tyrosine, low phenylalanine, and no tryptophan. In fact, 23 tyrosine residues are present in the S-layer protein and 14 of them are in the 123 residues of the C-terminal part. Tyrosines (TYR361, TYR391, TYR393, TYR426, TYR437) were predicted in the model structure to interact with carbohydrates, highlighted in blue in Fig. 7a. They correlate with the alignment of the proposed CRD described in GBP, ToxA, PCL, and MBL. To experimentally test the predicted model, tyrosine fluorescence quenching was assayed. We found that when increasing concentration of carbohydrates, a decrease in fluorescence is observed without changing the maximum emission and peak shape (Fig. 7b). Dissociation constants (K_d) were estimated for each reading. Comparative analysis for various carbohydrates enables to order them from highest to lowest affinity according to their estimated K_d (millimolar): D-lactose (44 ± 5 mM), *N*-acetylneuraminicacid (51 ± 5 mM), D-mannose (58 ± 6 mM), L-fucose (61 ± 6 mM), *N*-acetylglucosamine (71 ± 7 mM), glucosamine (98 ± 10 mM), D-glucose (106 ± 10 mM), and D-galactose (138 ± 11 mM). Chitin hydrolysate also showed a drastic decrease of fluorescence with increasing volume.

Discussion

This study was conceived to understand how the S-layer protein is anchored to the cell wall of *L. acidophilus* and how that

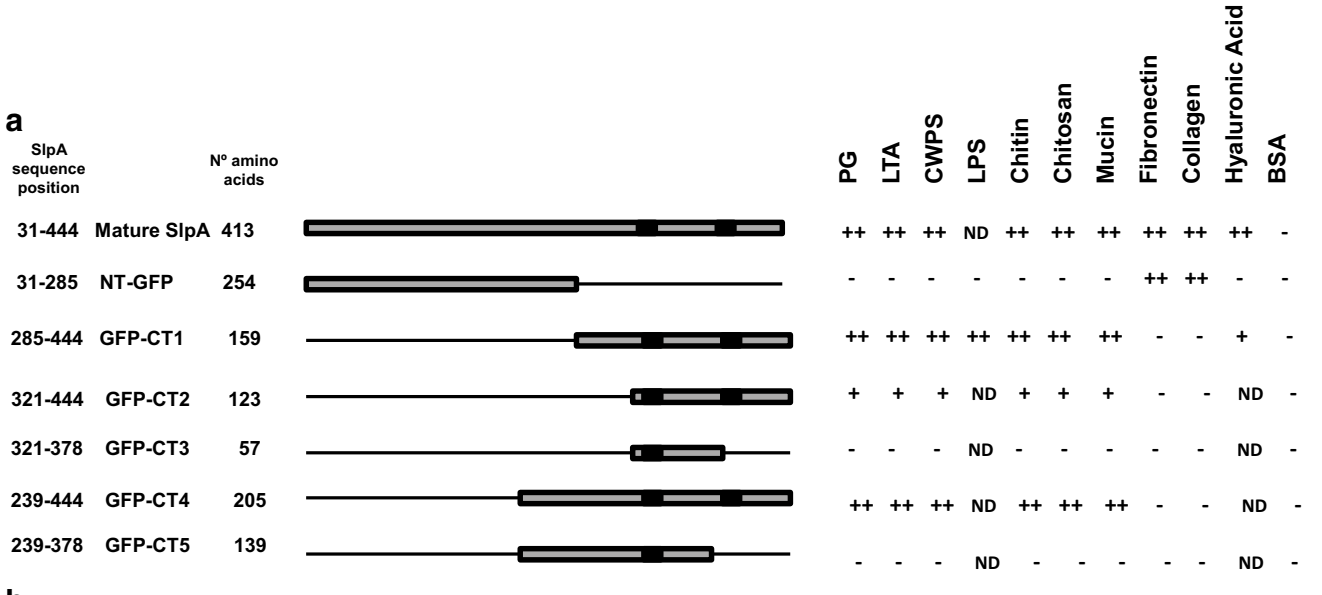

Fig. 4 **a** Interaction of mature SlpA and chimerical fusion proteins with different components. Prokaryotic cell wall components (PG, LTA, CWPS), eukaryotic macromolecules (mucin, fibronectin, collagen hyaluronic acid), and polymers (chitin and chitosan) were immobilized onto a PVDF membrane and were probed with mature SlpA or chimerical fluorescent fusion proteins. Carbohydrate recognition domains (CRD) are represented in black boxes. Plus and minus symbols indicate the level of interaction. ND not determined. **b** Multiple sequence alignment with hierarchical clustering using Multalin version 5.4.1 (http://multalin.toulouse.inra.fr/multalin/multalin.html) Sequence alignment of SlpA internal repeats IR1 (residues 322-378) and IR2 (residues 387-444). "|" identical aminoacid, ":" indicates group similarity, "." indicates low group similarity. Residues described in Fig. 7 are highlighted in blue for tyrosines or red for others. Sequons are those described for GBP and ToxA (von Eichel-Streiber et al. 1992) and PLC or MBL (An et al. 2006)

is related to the way it exerts its anti-microbial activity when used as a purified protein.

The interaction targets of S-layers were analyzed by means of the binding capacity to both prokaryotic and eukaryotic macromolecules. The S-layer has been proposed to bind to cell wall teichoic acid (Smit and Pouwels 2002; Antikainen et al. 2002; Åvall-Jääskeläinen et al. 2008) and more recently to lipoteichoic acid polymer (LTA) (Bönisch et al. 2018) when it is anchored to the cell. We found that it can also bind to other carbohydrate polymers as well, like chitin, when extracted and purified from the cells. We constructed chimerical fusion proteins to GFP with different parts of SlpA to determine its molecular interaction. We identified that the C-terminus binds to the cell wall of *L. acidophilus*, from which S-layer had been removed (Figs. 4 and 5). Furthermore, the binding of the C-terminus was abolished after treatment with LTA specific antibodies or with procedures that extract LTA (SDS) rather than those for PG-associated components, such as wall teichoic acids. These results suggest that lactobacillar surface proteins, which have a similar C-terminal sequence, interact by related mechanisms with the negatively charged teichoic acid on the bacterial surface, in accordance with the highly basic nature (*pI* = 10.00) of the C-terminal part of SlpA of *L. acidophilus*. Moreover, cationic peptides were shown to bind to LTA and to antagonize LTA-induced inflammatory effects (Scott et al. 1999), and the anchoring domains of several well-known teichoic acid or LTA-binding proteins are highly basic (Rigden et al. 2003).

As previously described (Smit et al. 2001), the GFP-CT1 was found to bind to the surface of *L. acidophilus*, but not to non-stripped cells or to *L. casei* (Fig. 6a). What are the

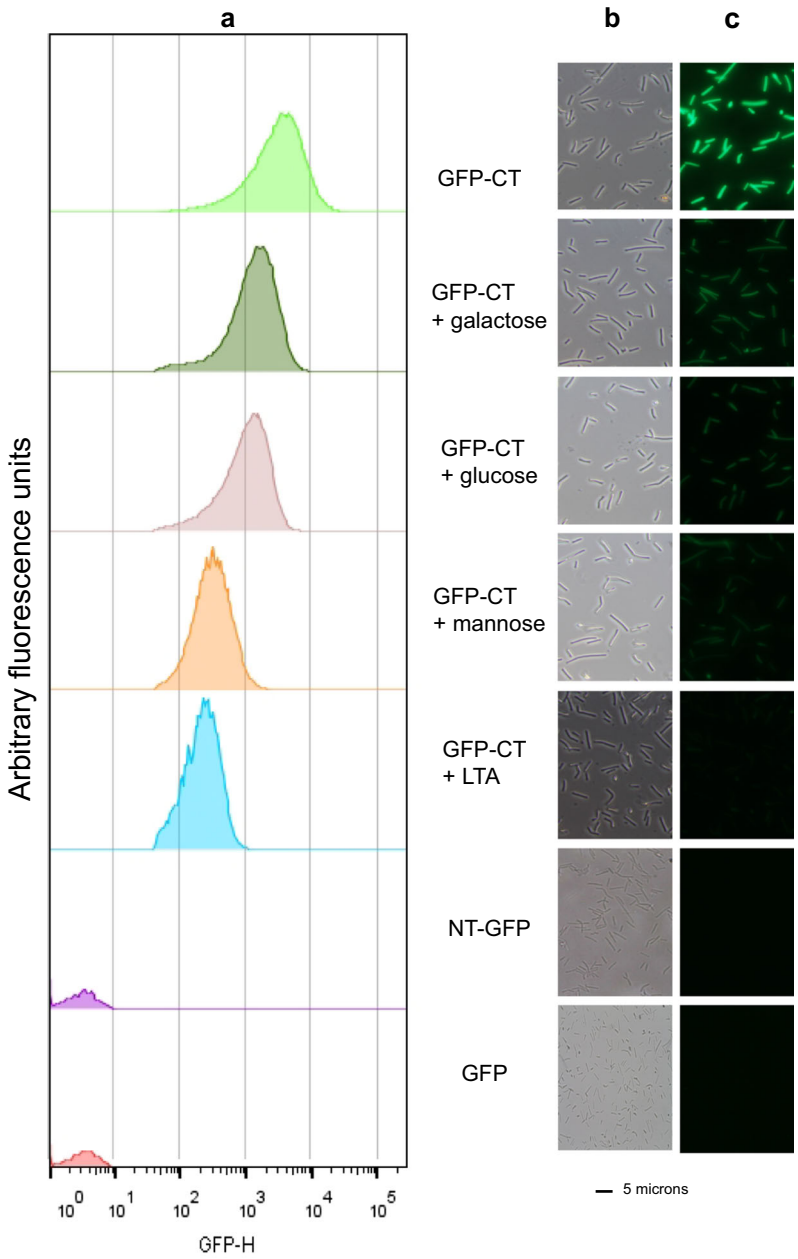
a
b
c
Arbitrary fluorescence units
GFP-CT
GFP-CT + galactose
GFP-CT + glucose
GFP-CT + mannose
GFP-CT + LTA
NT-GFP
GFP
10^0 10^1 10^2 10^3 10^4 10^5
GFP-H
5 microns

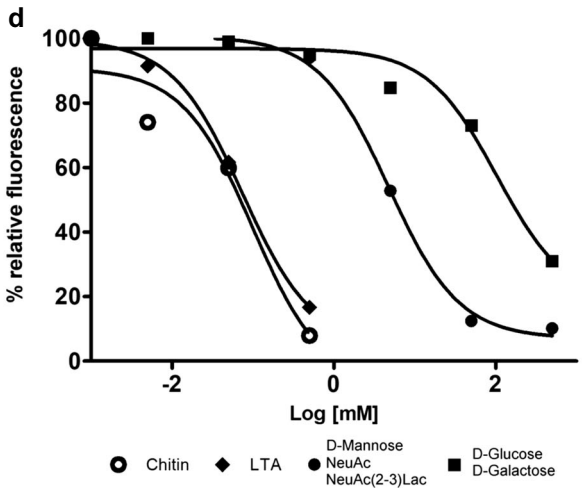
d
% relative fluorescence
100
80
60
40
20
0
-2
0
2
Log [mM]
Chitin
LTA
D-Mannose
NeuAc
NeuAc(2-3)Lac
D-Glucose
D-Galactose

◀ **Fig. 5** Binding inhibition of the C-terminal part of the SlpA protein to *Lactobacillus acidophilus* ATCC 4356 by carbohydrates was evaluated by flow cytometry (**a**) bright-light microscopy (**b**) and fluorescence microscopy (**c**). Magnification × 1000. GFP protein was used as negative control. (**d**) Inhibition curves are plotted. Calculated IC_{50} values are described in the text

differences between these two species other than having or not an S-layer protein? While *L. acidophilus* codes for *tag* genes which are responsible for the synthesis of WTA, *L. casei* does not (Altermann et al. 2005; Mazé et al. 2010; Palomino et al. 2015). In most Gram-positive bacteria, both LTAs and WTAs coexist, although certain bacterial species, including *L. casei* and *L. rhamnosus*, appear to contain only LTAs (Allievi et al. 2019). Analysis of LTA structures of lactic acid bacteria showed that the length of the Gro-P chains and the degree and composition of substitution as well as the nature of the glycolipid anchor is highly diverse and varies among species (Shiraishi et al. 2016). Another important difference involves the structure of the polyglycerol-phosphate in LTA with glycosylation and D-alanine; while *L. casei* is only substituted with D-alanine (Palomino et al. 2013; Allievi et al. 2019), glycosylation of the LTA molecules has been shown in several species but not yet in *L. acidophilus* (Shiraishi et al. 2016). In fact, structurally characterized LTA of *L. buchneri* CD034 shows the typical Gro-P backbone with glucose as the sole modification residue but not with D-alanine. Moreover, lactobacilli *dlt* mutants switched-off genes for D-alanylation and showed increased levels of glycosylation (Vélez et al. 2007). Whether glycosylation of LTA is involved in the S-layer recognition and attachment to the cell needs to be further investigated. Two observations support this as an attractive hypothesis:

1) Growth in high salt condition increases the release of S-layer protein from *L. acidophilus* cells (Palomino et al. 2016).

2) Binding of the GFP-CT1 decreased when pre-grown in high salt medium (Fig. 6b)

While increased glycosylation has been described for LTA of *Staphylococcus aureus* grown in high salt condition mediated by LTA specific glycosyltransferase, YfhO, that adds α-GlcNAc moieties to LTA (Kho and Meredith 2018), in *L. casei* a decreased polymer length was reported in high salt medium without glycosylation taking place (Palomino et al. 2013). Taking all these observations into account, low binding of GFP-CT1 to cells grown in high salt might indicate that glycosylation is reduced, in contrast to what is observed in *Staphylococcus*, or that the decreased polymer length is the reason for the increased release of the S-layer, in accordance with our previous findings in *L. casei*. Furthermore, it was found that in *Bacillus subtilis*, *csbB* and *yfhO* genes are essential for LTA glycosylation (Rismondo et al. 2018). Using bioinformatics analysis, we found that a *L. acidophilus* glycosyltransferase (WP-003547856, LBA1283 or NH13_RS06425, glycosyl transferase) (Altermann et al. 2005; Palomino et al. 2015) shows a clear homology to the *B. subtilis* CsbB protein. A detailed structure of the LTA of *L. acidophilus* is needed in order to answer these questions and will be the aim of our future work.

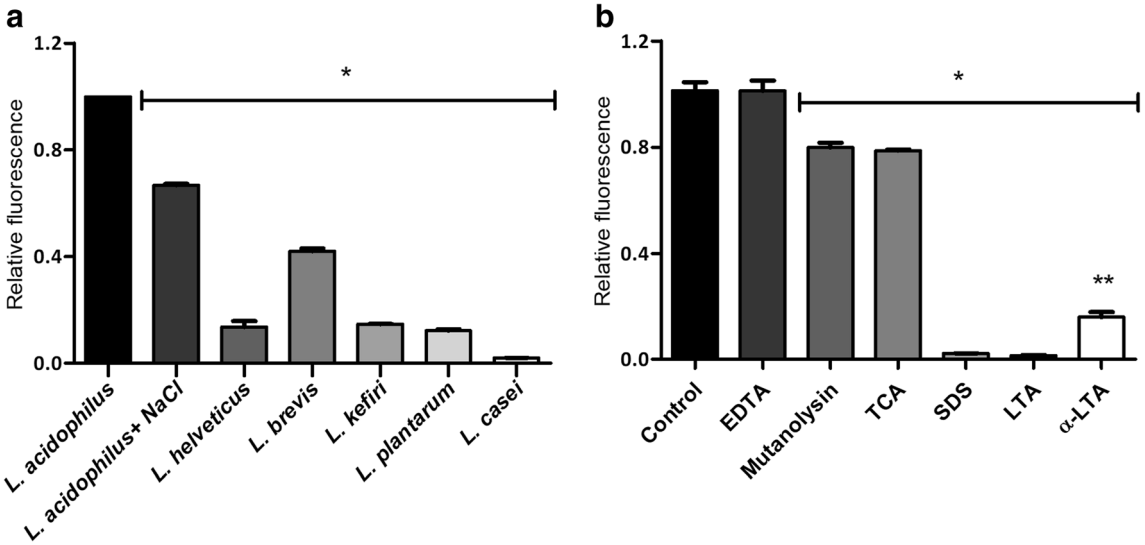

Fig. 6 Binding of the GFP-CT1 evaluated by flow cytometry: **a** to different *Lactobacillus* species and **b** to *L. acidophilus* cells treated with EDTA as chelating agent, TCA to remove WTA, mutanolysin to remove PG and WTA, and SDS to remove LTA. Purified LTA alone or pre-incubated with anti-LTA antibody were used as inhibitors of the binding of GFP-CT1. The asterisk (*) denotes significant difference with respect to the control **a** *L. acidophilus* cells or **b** with no treatment using the ANOVA method, Bonferroni test ($p < 0.05$). Double asterisk (**) denotes significant difference with respect to LTA inhibition for anti-LTA antibody preincubation using the ANOVA method, Bonferroni test ($p < 0.05$)

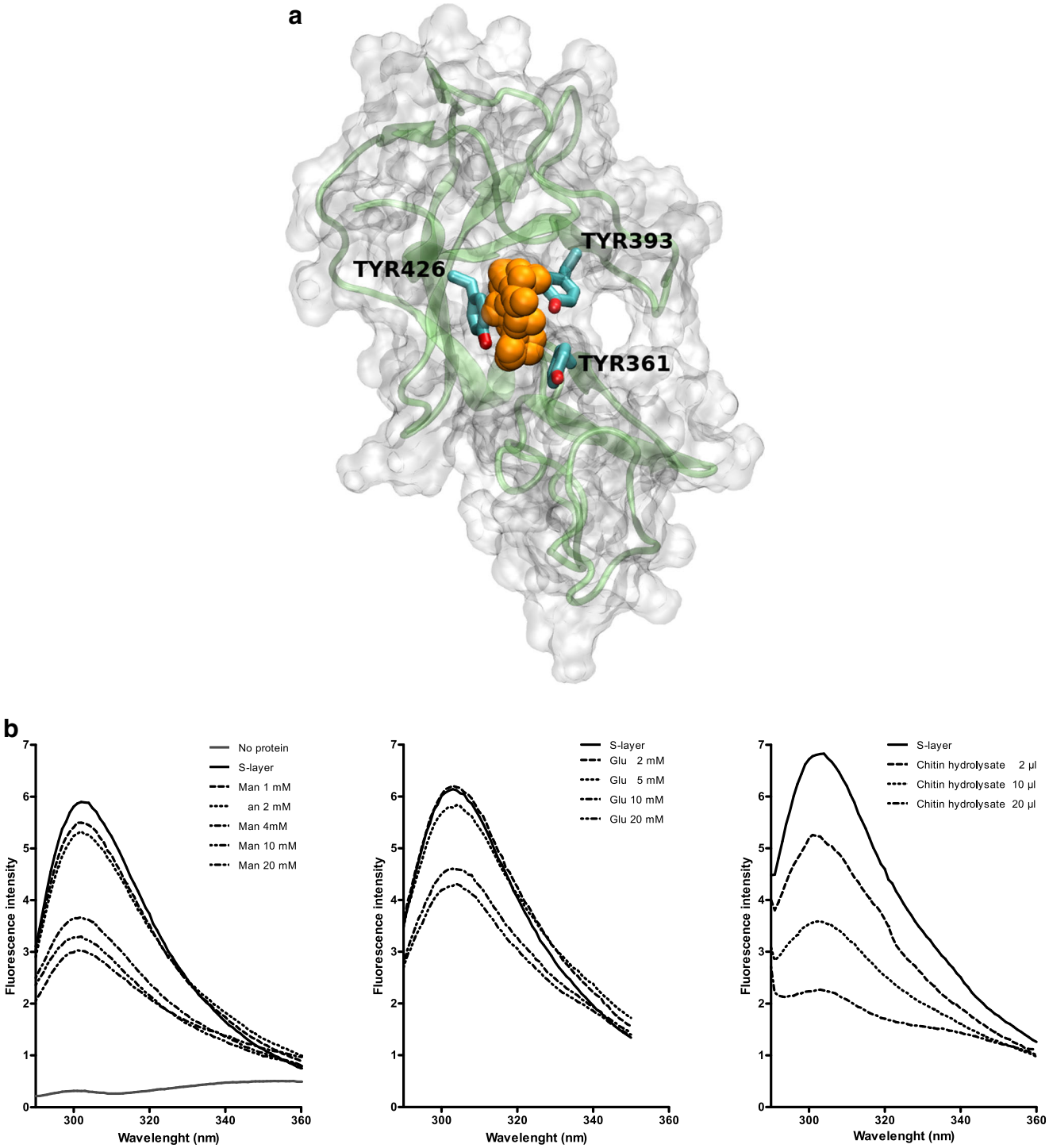

Fig. 7 **a** C-terminal structure prediction. The protein structure is shown as surface (transparent) and backbone (solid) representation, colored by green and gray respectively. The orange spheres represent the pocket cavity. Tyrosines predicted to interact with the ligand are colored by atom type (red, blue, cyan, and white for oxygen, nitrogen, carbon, and hydrogen, respectively). Residues that are components of the pocket: ASN351, **TYR361**, GLN362, VAL364, ALA390, TYR391, **TYR393**, GLN424, **TYR426**, TYR437, VAL438, LYS439 (tyrosines are shown in bold in the figure). **b** Fluorescence emission spectra of the S-layer was analyzed with increasing concentrations of carbohydrates. Three representative spectra are shown from three independent readings. The spectrum of the S-layer (0.5 mg/ml) is plotted without added carbohydrates. Man is for mannose and Glu for glucose in mM concentration. Chitin hydrolysate is indicated in the volume (µl.). No protein represents the spectrum of the maximum carbohydrate concentration tested

We found that the N-terminal part of SlpA shows affinity for collagen and fibronectin. This has been reported for the CbsA protein of *L. crispatus* and SlpA of *L. brevis*, which possess their adhesive domains in their N-terminal regions (Antikainen et al. 2002; Åvall-Jääskeläinen et al. 2008). Sequence variability is found in lactobacillar S-layer proteins even within the same species (Cavallero et al. 2017).

We confirmed that the S-layer protein of *L. acidophilus* ATCC 4356 is glycosylated as was shown for *L. acidophilus* NCFM strain and *L. helveticus* (Mozes et al. 1995; Konstantinov et al. 2008). A positive result was obtained in the lectin blot assay using ConA, a mannose-binding plant lectin that recognizes α-linked mannose residues of *N*-linked glycopeptides (asparagine linked), that are present as part of a "core oligosaccharide." Nine characteristic sequons (Asn-X-Ser/Thr) for *N*-linked oligosaccharides are predicted in the S-layer amino acid sequence, eight in the N-terminal and one in the C-terminal part of SlpA (Supplemental Fig. S3B). The presence of sequons for *N*-linked oligosaccharides in the N-terminal and only one in the C-terminal part of SlpA (Supplemental Fig. S3B) suggests that *N*-glycosylation of the S-layer mature protein is not involved in the interactions during carbohydrate recognition of the C-terminal part. No *O*-glycosylated peptide sequon (SSASSASSA), identified as a signature glycosylation motif in *L. buchneri* and *L. kefiri* (Anzengruber et al. 2014; Cavallero et al. 2017), is found in SlpA of *L. acidophilus.*

We established the minimum amino acid sequence required for binding to glycoconjugates from amino acid residues 321 to 444. We proposed that the S-layer protein lectin-like activity could in part explain its anti-microbial capacity and would provide biological benefits in the gastrointestinal tract functioning as a barrier to pathogens (Arena et al. 2017). Although Smit and Pouwels (2002) found that only one repeat of these two repeats is sufficient for anchoring the *L. acidophilus* surface layer protein to the cell wall in vitro, our results of binding in vivo showed that both repeats are necessary supporting a cooperative need of multiple binding sites like those found on ToxA or GBP proteins along the length of their carboxy termini, a feature that may strengthen binding to carbohydrates (Greco et al. 2006).

A structural model involving tyrosine residues in the interaction was predicted and experimentally verified. The volume of the pocket (564 Å) supports the idea of interaction with sugar decorating macromolecules, like glycosylation of LTA or in glycoproteins. However, these predictions lack confirmation because of the impossibility of obtaining the crystallization of the protein for X-ray diffraction analysis. No three-dimensional structure of *Lactobacillus* S-layer proteins has been solved yet. Crystallization or NMR are needed in order to be able to elucidate the molecular mechanism of interaction with carbohydrates or other macromolecules and will be the aim of our future work.

A wide range of binding preferences is observed for the *L. acidophilus* ATCC 4356 S-layer protein. SlpA shows lectin activity preferences for polymeric rather than oligomeric carbohydrates. The chitin-binding activity is similar to hevein-type lectins such as wheat germ *Triticum vulgare* (WGA) that can bind oligosaccharides that contain terminal N-acetylglucosamine, as is the case of PG and chitin, and interact with some glycoproteins via terminal sialic acid (Itakura et al. 2017; Leyva et al. 2019). The capacity of SlpA to bind chitin and chitosan could correlate with other activities described for *L. acidophilus*, including the capacity to hydrolyze chitin (Palomino et al. 2015). Correlation was found for the ability to metabolize these monosaccharides by metabolic profiling in fermentation medium, although no correlation was observed when using intact polymers (chitin) or proteins (mucin) as substrates, probably due to the low concentrations that we can test in vitro (data not shown). In fact, functions related to chitin, *N*-acetylglucosamine utilization and sialic acid catabolism are found in *L. acidophilus* genomes which include a PTS transport system and catabolic activities (Altermann et al. 2005; Palomino et al. 2015). Since neither *N*-acetylneuraminic acid (Neu5Ac), the most common sialic acid, nor any of its numerous structural derivatives are synthesized by most nonpathogenic Bacteria, the presence of catabolic genes shows a direct correlation with it probably being a nutrient source.

Binding also resembles that of mannose/sialic acid-binding protein lectins, i.e., *Polygonatum cyrtonema* Hua lectin (PCL, GenBank Accession No. AAM28644) described to have anti-HIV activity (An et al. 2006), although with less affinity. In fact, PCL mature polypeptide contained three tandemly arranged sequons (Q-D-N-V-Y), with sequence homology to mannose-binding lectins (MBL) as well as three sialic acid-binding regions. A putative similarity was found in the internal repeats of the C-terminal part of SlpA (Fig. 4b).

L. acidophilus slpA knockouts show diminished adhesion to mucus in vitro (Buck et al. 2005). Interaction with mucin-bound *O*-glycans during bacterial infection mediates pathogen adhesion to epithelial cells via carbohydrate-lectin interactions and acts as cytoprotective by capturing the pathogen in the mucin gel. Moreover, mucin-bound *O*-glycans are considered to be nutrients for commensal bacteria (van Tassell and Miller 2011). The agglutinating capacity of the S-layer to bacterial cells and virus particles would act in a similar way to capture pathogens and provide lactobacilli to interact with mucin glycans.

Mannose binding was corroborated by the finding that it inhibited hemagglutination and that S-layer protein has the capacity to agglutinate *S. cerevisiae*. Low affinity interactions with D-mannose was observed, but notably, no interaction with RNAse B or glucose oxidase, both glycoproteins containing high mannose *N*-glycans. These results may reflect a specific affinity for mannose residues with linkages that are not present or exposed in these *N*-glycans. Mannose-binding lectins are proteins of the innate immune system, able to

recognize and bind various pathogens (including bacteria, viruses, fungi, and parasites), providing protection against the microbial invasion of the host (Auriti et al. 2017; Coelho et al. 2018). Competitive exclusion strategies for pathogens displaying mannose residues on their cell surfaces such as *Candida albicans*, at mannose-containing receptors on the epithelial surface, are interesting as anti-microbial perspectives (Hammad et al. 2018). Therefore, the presence of a mannose-binding capacity of the S-layer protein could be used as a possible way to conform a GRAS (generally regarded as save) status barrier using the purified S-layer as an additive to probiotic formulations. In fact, immunomodulatory effects of the purified S-layer protein, able to induce cytokine production in culture cells, have also been found (Konstantinov et al. 2008; Coelho et al. 2018). Considering both the immunomodulatory effect and the anchor capacity of the C-terminal part, surface display strategies without genetic modification for anchoring antigens to NaCl treated cells is a good way for developing non-genetically modified organism (non-GMO) formulations for oral vaccines (Sahay et al. 2015) as those employing S-layer proteins (Mao et al. 2016). Also, the interaction with viruses to reduce viral titer might be a good strategy to reduce viral infections, as those that are being studied by others with lectins as anti-HIV approach (Akkouh et al. 2015).

In summary, we have experimentally shown that SlpA is able to recognize carbohydrate derivatives, with preference for polymeric structures as shown for other lectins (Bose et al. 2016; Patel et al. 2016). This lectin activity makes it possible to propose a mechanism for the immunomodulatory, anti-viral, and anti-bacterial properties reported for this protein.

Acknowledgments We are very grateful to Carmen Sanchez-Rivas for the helpful discussions.

Funding This work was supported by grants from the Universidad de Buenos Aires and the CONICET Argentina to SMR. JFM is a graduate fellow of CONICET.

Compliance with ethical standards

Conflict of interest The authors declare that they have no competing interests.

Ethical approval This article does not contain any studies with human participants or animals performed by any of the authors.

References

Akkouh O, Ng TB, Singh SS, Yin C, Dan X, Chan YS, Pan W, Cheung RCF (2015) Lectins with anti-HIV activity: a review. Molecules 20:648–668. https://doi.org/10.3390/molecules20010648

Allievi MC, Palomino MM, Prado Acosta M, Lanati L, Ruzal SM, Sánchez-Rivas C (2014) Contribution of S-layer proteins to the mosquitocidal activity of *Lysinibacillus sphaericus*. PLoS One 9: 111114. https://doi.org/10.1371/journal.pone.0111114

Allievi MC, Ruzal SM, Palomino MM (2019) Modifications of *Lactobacillus* surface under environmental stress conditions. In: Ruzal SM (ed) *Lactobacillus* genomics and metabolic engineering. Caister Academic Press, Wymondham, Norfolk, UK, pp 81–103. https://doi.org/10.21775/9781910190890

Altermann E, Russell WM, Azcarate-Peril MA, Barrangou R, Buck BL, McAuliffe O, Souther N, Dobson A, Duong T, Callanan M, Lick S, Hamrick A, Cano R, Klaenhammer TR (2005) Complete genome sequence of the probiotic lactic acid bacterium *Lactobacillus acidophilus* NCFM. Proc Natl Acad Sci U S A 102:3906–3912. https://doi.org/10.1073/pnas.0409188102

Alva V, Nam S-Z, Söding J, Lupas AN (2016) The MPI bioinformatics toolkit as an integrative platform for advanced protein sequence and structure analysis. Nucleic Acids Res 44:410–415. https://doi.org/10.1093/nar/gkw348

An J, Liu JZ, Wu CF, Li J, Dai L, Van Damme E, Balzarini J, De Clercq E, Chen F, Bao JK (2006) Anti-HIV I/II activity and molecular cloning of a novel mannose/sialic acid-binding lectin from rhizome of *Polygonatum cyrtonema* Hua. Acta Biochim Biophys Sin Shanghai 38:70–78. https://doi.org/10.1111/j.1745-7270.2006.00140.x

Antikainen J, Anton L, Sillanpää J, Korhonen TK (2002) Domains in the S-layer protein CbsA of *Lactobacillus crispatus* involved in adherence to collagens, laminin and lipoteichoic acids and in self-assembly. Mol Microbiol 46:381–394. https://doi.org/10.1046/j.1365-2958.2002.03180.x

Anzengruber J, Pabst M, Neumann L, Sekot G, Heinl S, Grabherr R, Altmann F, Messner P, Schäffer C (2014) Protein *O*-glucosylation in *Lactobacillus buchneri*. Glycoconj J 31:117–131. https://doi.org/10.1007/s10719-013-9505-7

Arena MP, Capozzi V, Spano G, Fiocco D (2017) The potential of lactic acid bacteria to colonize biotic and abiotic surfaces and the investigation of their interactions and mechanisms. Appl Microbiol Biotechnol 101:2641–2657. https://doi.org/10.1007/s00253-017-8182-z

Ashida N, Yanagihara S, Shinoda T, Yamamoto N (2011) Characterization of adhesive molecule with affinity to Caco-2 cells in *Lactobacillus acidophilus* by proteome analysis. J Biosci Bioeng 112:333–337. https://doi.org/10.1016/j.jbiosc.2011.06.001

Auriti C, Prencipe G, Moriondo M, Bersani I, Bertaina C, Mondì V, Inglese R (2017) Mannose-binding lectin: biologic characteristics and role in the susceptibility to infections and ischemia-reperfusion related injury in critically ill neonates. J Immunol Res 2017:1–11. https://doi.org/10.1155/2017/7045630

Åvall-Jääskeläinen S, Lindholm A, Palva A (2003) Surface display of the receptor-binding region of the *Lactobacillus brevis* S-layer protein in *Lactococcus lactis* provides nonadhesive lactococci with the ability to adhere to intestinal epithelial cells. Appl Environ Microbiol 69:2230–2236

Åvall-Jääskeläinen S, Hynönen U, Ilk N, Pum D, Sleytr UB, Palva A (2008) Identification and characterization of domains responsible for self-assembly and cell wall binding of the surface layer protein of *Lactobacillus brevis* ATCC 8287. BMC Microbiol 8:165. https://doi.org/10.1186/1471-2180-8-165

Blackler RJ, López-Guzmán A, Hager FF, Janesch B, Martinz G, Gagnon SML, Haji-ghassemi O, Kosma P, Messner P, Schäffer C, Evans SV (2018) Structural basis of cell wall anchoring by SLH domains in *Paenibacillus alvei*. Nat Commun 9:3120. https://doi.org/10.1038/s41467-018-05471-3

Blanco Capurro JI, Di Paola M, Gamarra MD, Martí MA, Modenutti CP (2019) An efficient use of X-ray information, homology modeling,

molecular dynamics and knowledge-based docking techniques to predict protein-monosaccharide complexes. Glycobiol 29:124–136. https://doi.org/10.1093/glycob/cwy102

Blanco Fernández MD, Barrios ME, Cammarata RV, Torres C, Taboga OA, Mbayed VA (2017) Comparison of internal process control viruses for detection of food and waterborne viruses. Appl Microbiol Biotechnol 101:4289–4298. https://doi.org/10.1007/s00253-017-8244-2

Bönisch E, Oh YJ, Anzengruber J, Hager FF, López-Guzmán A, Zayni S, Hinterdorfer P, Kosma P, Messner P, Duda KA, Schäffer C (2018) Lipoteichoic acid mediates binding of a *Lactobacillus* S-layer protein. Glycobiology 28:148–158. https://doi.org/10.1093/glycob/cwx102

Bose PP, Bhattacharjee S, Singha S, Mandal S, Mondal G, Gupta P, Chatterjee BP (2016) A glucose/mannose binding lectin from litchi (*Litchi chinensis*) seeds: biochemical and biophysical characterizations. Biochem Biophys Reports 6:242–252. https://doi.org/10.1016/j.bbrep.2016.05.001

Buck BL, Altermann E, Svingerud T, KlaenhammerTR (2005) Functional Analysis of Putative Adhesion Factors in *Lactobacillus acidophilus* NCFM. App Environ Microbiol 71:8344–8351. https://doi.org/10.1128/AEM.71.12.8344-8351.2005

Carasi P, Ambrosis NM, De Antoni GL, Bressollier P, Urdaci MC, Serradell MA (2014) Adhesion properties of potentially probiotic *Lactobacillus kefiri* to gastrointestinal mucus. J Dairy Res 81:16–23. https://doi.org/10.1017/S0022029913000526

Cavallero GJ, Malamud M, Casabuono AC, Serradell MA, Couto AS (2017) A glycoproteomic approach reveals that the S-layer glycoprotein of *Lactobacillus kefiri* CIDCA 83111 is *O*- and *N*-glycosylated. J Proteome 162:20–29. https://doi.org/10.1016/j.jprot.2017.04.007

Cleveland RF, Holtje J-V, Wicken AJ, Tomasz A, Daneo-Moore L, Shockman GD (1975) Inhibition of bacterial wall lysins by lipoteichoic acids and related compounds. Biochem Biophys Res Commun 67:1128–1135. https://doi.org/10.1016/0006-291X(75)90791-3

Coelho LCBB, dos Santos Silva PM, Oliveira WF, Moura MC, Pontual EV, Gomes FS, Paiva PMG, Napoleão TH, dos Santos Correia MT (2018) Lectins as antimicrobial agents. J Appl Microbiol 125:1238–1252. https://doi.org/10.1111/jam.14055

de Ambrosini VM, Gonzalez S, Perdigon G, Holgado APDR, Oliver G (1996) Chemical composition of the cell wall of lactic acid bacteria and related species. Chem Pharm Bull (Tokyo) 44:2263–2267. https://doi.org/10.1248/cpb.44.2263

Dieterle ME, Bowman C, Batthyany C, Lanzarotti E, Turjanski A, Hatfull G, Piuri M (2014) Exposing the secrets of two well-known *Lactobacillus casei* phages, J-1 and PL-1, by genomic and structural analysis. Appl Environ Microbiol 80:7107–7121. https://doi.org/10.1128/AEM.02771-14

do Carmo FLR, Rabah H, De Oliveira Carvalho RD, Gaucher F, Cordeiro BF, da Silva SH, Le Loir Y, Azevedo V, Jan G (2018) Extractable bacterial surface proteins in probiotic–host interaction. Front Microbiol 9:645. https://doi.org/10.3389/fmicb.2018.00645

Domurado M, Domurado D, Vansteenkiste S, De Marre A, Schacht E (1995) Glucose oxidase as a tool to study in vivo the interaction of glycosylated polymers with the mannose receptor of macrophages. J Control Release 33:115–123. https://doi.org/10.1016/0168-3659(94)00074-5

Eswar N, Eramian D, Webb B, Shen M-Y, Sali A (2008) Protein structure modeling with MODELLER. In: Kobe B, Guss M, Huber T (eds) Structural proteomics. Methods in Molecular Biology™, vol 426. Humana Press, CBS Publishers, New Delhi, India, pp 145–159. https://doi.org/10.1007/978-1-60327-058-8_8

Greco A, Ho JGS, Lin S, Palcic MM, Rupnik M, Ng KK-S (2006) Carbohydrate recognition by *Clostridium difficile* toxin A. Nat Struct Mol Biol 13:460–461. https://doi.org/10.1038/nsmb1084

Hammad NM, El Badawy NE, Ghramh HA, Al KadyLM (2018) Mannose-Binding Lectin: A Potential Therapeutic Candidate against Infection. BioMed Research International 2018:1–8. https://doi.org/10.1155/2018/2813737

Ho JGS, Greco A, Rupnik M, Ng KK-S (2005) Crystal structure of receptor-binding C-terminal repeats from *Clostridium difficile* toxin A. Proc Natl Acad Sci 102:18373–18378. https://doi.org/10.1073/pnas.0506391102

Howling GI, Dettmar PW, Goddard PA, Hampson FC, Dornish M, Wood EJ (2001) The effect of chitin and chitosan on the proliferation of human skin fibroblasts and keratinocytes in vitro. Biomaterials 22:2959–2966. https://doi.org/10.1016/S0142-9612(01)00042-4

Hymes JP, Klaenhammer TR (2016) Stuck in the middle: fibronectin-binding proteins in Gram-positive bacteria. Front Microbiol 7:1–9. https://doi.org/10.3389/fmicb.2016.01504

Hynönen U, Kant R, Lähteinen T, Pietilä TE, Beganović J, Smidt H, Uroić K, Åvall-Jääskeläinen S, Palva A (2014) Functional characterization of probiotic surface layer protein-carrying *Lactobacillus amylovorus* strains. BMC Microbiol 14:199. https://doi.org/10.1186/1471-2180-14-199

Itakura Y, Nakamura-Tsuruta S, Kominami J, Tateno H, Hirabayashi J (2017) Sugar-binding profiles of chitin-binding lectins from the Hevein family: a comprehensive study. Int J Mol Sci 18:1160. https://doi.org/10.3390/ijms18061160

Janesch B, Messner P, Schäffer C (2013) Are the surface layer homology domains essential for cell surface display and glycosylation of the S-layer protein from *Paenibacillus alvei* CCM 2051T? J Bacteriol 195:565–575. https://doi.org/10.1128/JB.01487-12

Johnson B, Selle K, O'Flaherty S, Goh YJ, Klaenhammer T (2013) Identification of extracellular surface-layer associated proteins in *Lactobacillus acidophilus* NCFM. Microbiol (United Kingdom) 159:2269–2282. https://doi.org/10.1099/mic.0.070755-0

Kho K, Meredith TC (2018) Salt-induced stress stimulates a lipoteichoic acid-specific three component glycosylation system in *Staphylococcus aureus*. J Bacteriol 200:e00017–e00018. https://doi.org/10.1128/JB.00017-18

Konstantinov SR, Smidt H, De VWM, Bruijns SCM, Kaur S, Valence F, Molle D, Lortal S, Altermann E, Klaenhammer TR, Van KY (2008) S layer protein A of *Lactobacillus acidophilus* NCFM regulates immature dendritic cell and T cell functions. Proc Natl Acad Sci U S A 105:19474–19479. https://doi.org/10.1073/pnas.0810305105

Le Guilloux V, Schmidtke P, Tuffery P (2009) Fpocket: an open source platform for ligand pocket detection. BMC Bioinformatics 10:168. https://doi.org/10.1186/1471-2105-10-168

Leyva E, Medrano-Cerano JL, Cano-Sánchez P, Gómez-Velasco H, Del Río-Portilla P, García-Hernández E (2019) Bacterial expression, purification and biophysical characterization of wheat germ agglutinin and its four hevein-like domains. Biopolymers 110:23242. https://doi.org/10.1002/bip.23242

Malamud M, Bolla PA, Carasi P, Gerbino E, Gómez-Zavaglia A, Mobili P, de los Angeles Serradell M (2019) S-Layer proteins from Lactobacilli: biogenesis, structure, functionality and biotechnological applications. In: Ruzal SM (ed) *Lactobacillus* genomics and metabolic engineering. Caister Academic Press, Wymondham, Norfolk, UK, pp 105–129. https://doi.org/10.21775/9781910190890

Mao R, Wu D, Wang Y (2016) Surface display on lactic acid bacteria without genetic modification: strategies and applications. Appl Microbiol Biotechnol 100:9407–9421. https://doi.org/10.1007/s00253-016-7842-8

Martínez MG, Prado Acosta M, Candurra NA, Ruzal SM (2012) S-layer proteins of *Lactobacillus acidophilus* inhibits JUNV infection. Biochem Biophys Res Commun 422:590–595. https://doi.org/10.1016/j.bbrc.2012.05.031

Mazé A, Boël G, Zúñiga M, Bourand A, Loux V, Yebra MJ, Monedero V, Correia K, Jacques N, Beaufils S, Poncet S, Joyet P, Milohanic E, Casarégola S, Auffray Y, Pérez-Martínez G, Gibrat J-F, Zagorec M, Francke C, Hartke A, Deutscher J (2010) Complete genome sequence of the probiotic *Lactobacillus casei* strain BL23. J Bacteriol 192:2647–2648. https://doi.org/10.1128/JB.00076-10

Meng J, Gao S-M, Zhang Q-X, Lu R-R (2015) Murein hydrolase activity of surface layer proteins from *Lactobacillus acidophilus* against *Escherichia coli*. Int J Biol Macromol 79:527–532. https://doi.org/10.1016/j.ijbiomac.2015.03.057

Mozes N, Lortal S, Lotta S (1995) X-ray photoelectron spectroscopy and biochemical analysis of the surface of *Lactobacillus helveticus* ATCC 12046. Microbiology 141:11–19

Naughton JA, Mariño K, Dolan B, Reid C, Gough R, Gallagher ME, Kilcoyne M, Gerlach JQ, Joshi L, Rudd P, Carrington S, Bourke B, Clyne M (2013) Divergent mechanisms of interaction of *Helicobacter pylori* and *Campylobacter jejuni* with mucus and mucins. Infect Immun 81:2838–2850. https://doi.org/10.1128/IAI.00415-13

Nishiyama K, Sugiyama M, Mukai T (2016) Adhesion properties of lactic acid bacteria on intestinal mucin. Microorganisms 4:34. https://doi.org/10.3390/microorganisms4030034

Palomino MM, Allievi MC, Gründling A, Sanchez-Rivas C, Ruzal SM (2013) Osmotic stress adaptation in *Lactobacillus casei* BL23 leads to structural changes in the cell wall polymer lipoteichoic acid. Microbiol (United Kingdom) 159:2416–2426. https://doi.org/10.1099/mic.0.070607-0

Palomino MM, Allievi MC, Fina Martin J, Waehner PM, Prado Acosta M, Sanchez Rivas CS, Ruzal SM (2015) Draft genome sequence of the probiotic strain *Lactobacillus acidophilus* ATCC 4356. Genome Announc 3(1):01421–01414. https://doi.org/10.1128/genomeA.01421-14

Palomino MM, Waehner PM, Fina Martin J, Ojeda P, Malone L, Sánchez Rivas C, Prado Acosta M, Allievi MC, Ruzal SM (2016) Influence of osmotic stress on the profile and gene expression of surface layer proteins in *Lactobacillus acidophilus* ATCC 4356. Appl Microbiol Biotechnol 100:8475–8484. https://doi.org/10.1007/s00253-016-7698-y

Panwar R, Kumar N, Kashyap V, Singh S, Singh H (2017) Insights into involvement of S-layer proteins of probiotic Lactobacilli in relation to gut health. Oct Jour Env Res 5:228–245

Patel DK, Shah KR, Pappachan A, Gupta S, Singh DD (2016) Cloning, expression and characterization of a mucin-binding GAPDH from *Lactobacillus acidophilus*. Int J Biol Macromol 91:338–346. https://doi.org/10.1016/j.ijbiomac.2016.04.041

Piuri M, Sanchez-Rivas C, Ruzal SM (2005) Cell wall modifications during osmotic stress in *Lactobacillus casei*. J Appl Microbiol 98:84–95. https://doi.org/10.1111/j.1365-2672.2004.02428.x

Piuri M, Jacobs WR, Hatfull GF (2009) Fluoromycobacteriophages for rapid, specific, and sensitive antibiotic susceptibility testing of *Mycobacterium tuberculosis*. PLoS One 4:4870. https://doi.org/10.1371/journal.pone.0004870

Prado Acosta M, Mercedes Palomino M, Allievi MC, Sanchez Rivas C, Ruzal SM (2008) Murein hydrolase activity in the surface layer of *Lactobacillus acidophilus* ATCC 4356. Appl Environ Microbiol 74:7824–7827. https://doi.org/10.1128/AEM.01712-08

Prado Acosta M, Ruzal SM, Cordo SM (2016) S-layer proteins from *Lactobacillus* sp. inhibit bacterial infection by blockage of DC-SIGN cell receptor. Int J Biol Macromol 92:998–1005. https://doi.org/10.1016/j.ijbiomac.2016.07.096

Prado-Acosta M, Ruzal SM, Allievi MC, Palomino MM, Sanchez Rivas C (2010) Synergistic effects of the *Lactobacillus acidophilus* surface layer and nisin on bacterial growth. Appl Environ Microbiol 76:974–977. https://doi.org/10.1128/AEM.01427-09

Rigden DJ, Galperin MY, Jedrzejas MJ (2003) Analysis of structure and function of putative surface-exposed proteins encoded in the *Streptococcus pneumoniae* genome: a bioinformatics-based approach to vaccine and drug design. Crit Rev Biochem Mol Biol 38:143–168. https://doi.org/10.1080/713609215

Rismondo J, Percy MG, Gründling A (2018) Discovery of genes required for lipoteichoic acid glycosylation predicts two distinct mechanisms for wall teichoic acid glycosylation. J Biol Chem 293:3293–3306. https://doi.org/10.1074/jbc.RA117.001614

Sahay B, Ge Y, Colliou N, Zadeh M, Weiner C, Mila A, Owen JL, Mohamadzadeh M (2015) Advancing the use of *Lactobacillus acidophilus* surface layer protein a for the treatment of intestinal disorders in humans. Gut Microbes 6:392–397. https://doi.org/10.1080/19490976.2015.1107697

Sano K, Ogawa H (2014) Hemagglutination (inhibition) assay. In: Hirabayashi J (ed) Lectins. Methods in molecular biology (methods and protocols), vol 1200. Humana Press, New York, NY, pp 47–52. https://doi.org/10.1007/978-1-4939-1292-6_4

Scott MG, Gold MR, Hancock RE (1999) Interaction of cationic peptides with lipoteichoic acid and gram-positive bacteria. Infect Immun 67:6445–6453

Shiraishi T, Yokota S-I, Fukiya S, Yokota A (2016) Structural diversity and biological significance of lipoteichoic acid in Gram-positive bacteria: focusing on beneficial probiotic lactic acid bacteria. Biosci Microbiota Food Health 35:147–161. https://doi.org/10.12938/bmfh.2016-006

Sleytr UB, Schuster B, Egelseer EM, Pum D (2014) S-layers: principles and applications. FEMS Microbiol Rev 38:823–864. https://doi.org/10.1111/1574-6976.12063

Smit E, Pouwels PH (2002) One repeat of the cell wall binding domain is sufficient for anchoring the *Lactobacillus acidophilus* surface layer protein. J Bacteriol 184:4617–4619. https://doi.org/10.1128/JB.184.16.4617-4619.2002

Smit E, Oling F, Demel R, Martinez B, Pouwels PH (2001) The S-layer protein of *Lactobacillus acidophilus* ATCC 4356: identification and characterisation of domains responsible for S-protein assembly and cell wall binding. J Mol Biol 305:245–257. https://doi.org/10.1006/jmbi.2000.4258

Sosa EJ, Burguener G, Lanzarotti E, Defelipe L, Radusky L, Pardo AM, Marti M, Turjanski AG, Fernández Do Porto D (2018) Target-pathogen: a structural bioinformatic approach to prioritize drug targets in pathogens. Nucleic Acids Res 46:413–418. https://doi.org/10.1093/nar/gkx1015

Suhr M, Lederer FL, Günther TJ, Raff J (2016) Characterization of three different unusual S-layer proteins from *Viridibacillus arvi* JG-B58 that exhibits two super-imposed S-layer proteins. PLoS One 11:0156785. https://doi.org/10.1371/journal.pone.0156785

van Tassell ML, Miller MJ (2011) *Lactobacillus* adhesion to mucus. Nutrients 3:613–636. https://doi.org/10.3390/nu3050613

Vélez MP, Verhoeven TLA, Draing C, Von Aulock S, Pfitzenmaier M, Geyer A, Lambrichts I, Grangette C, Pot B, Vanderleyden J, De Keersmaecker SCJ (2007) Functional analysis of D-alanylation of lipoteichoic acid in the probiotic strain *Lactobacillus rhamnosus* GG. Appl Environ Microbiol 73:3595–3604. https://doi.org/10.1128/AEM.02083-06

von Eichel-Streiber C, Sauerborn M, Kuramitsu HK (1992) Evidence for a modular structure of the homologous repetitive C-terminal carbohydrate-binding sites of *Clostridium difficile* toxins and *Streptococcus mutans* glucosyltransferases. J Bacteriol 174:6707–6710

Windwarder M, Altmann F (2014) Site-specific analysis of the *O*-glycosylation of bovine fetuin by electron-transfer dissociation mass

spectrometry. J Proteome 108:258–268. https://doi.org/10.1016/j.jprot.2014.05.022

Zhu C, Guo G, Ma Q, Zhang F, Ma F, Liu J, Xiao D, Yang X, Sun M (2016) Diversity in S-layers. Prog Biophys Mol Biol 123:1–15. https://doi.org/10.1016/j.pbiomolbio.2016.08.002

Zoll S, Schlag M, Shkumatov AV, Rautenberg M, Svergun DI, Götz F, Stehle T (2012) Ligand-binding properties and conformational dynamics of autolysin repeat domains in staphylococcal cell wall recognition. J Bacteriol 194:3789–3802. https://doi.org/10.1128/JB.00331-12